Histol Histopathol (2024) 39: 1597-1610

Histology and Histopathology
From Cell Biology to Tissue Engineering

ORIGINAL ARTICLE Open Access

Histopathological and statistical study of corneal repair in rabbits. A new way to understand corneal recovery

Patricia Ramírez-Perdomo[1], Juan Daniel Hernández-Marrero[2], Santiago Guillén-Molina[3], Pedro Saavedra-Santana[4], Mónica de León-Vera[5], Eduardo José Araujo-Ruano[1], Juan Francisco Loro-Ferrer[6], Juan José Cabrera-Galván[1] and Juan Andrés Ramírez-González[1]

[1]Morphology Department, Las Palmas de Gran Canaria University (ULPGC), [2]Exotics Animal´s Veterinary Service (Serviexotic), [3]Albion Ophthalmological Clinic, [4]Mathematics Department, Las Palmas de Gran Canaria University (ULPGC), [5]Veterinary Specialities (OFTALVET) and [6]Clinical Sciences Department, Las Palmas de Gran Canaria University, Gran Canaria, Spain

Summary. The study aims to evaluate corneal healing post amniotic membrane transplantation in controlled corneal defects, justifying its application in routine ophthalmology practice. The objective is to establish a reliable method for assessing the repair process.

In three groups of six adult New Zealand rabbits, keratectomy and a monolayer transplant of dehydrated human amniotic membrane (AM) were conducted in the left eye (OS) with the right eye (OD) serving as the control eye. Clinical signs were assessed, and both eyes were enucleated at 1, 2, and 4 weeks for optical coherence tomography (OCT) measurements and histological analysis, collecting data from different epithelium, stroma, and limbus regions. This study was conducted using a formula that combines histologic data categorizing their presence and/or type as beneficial for corneal repair.

No statistically significant differences were found between the experimental and control eyes regarding all clinical signs and OCT measurements. However, a linear model using histopathological results showed a period-implant mode interaction with statistical significance (P=0.010).

The use of the single-layer amniotic membrane resulted in improved corneal recovery with the stromal side showing better performance in the first week and the epithelial side proving to be more effective than the stromal side in the long term. For the first time, a statistical formula employing histopathological data is introduced to determine corneal recovery, potentially offering a more accurate and reliable method compared with the observation of clinical signs and corneal measurements with OCT.

Corresponding Author: Juan José Cabrera-Galván, Avda. Blas Cabrera Felipe s/n, Facultad de Medicina, 35016 Las Palmas de Gran Canaria, Spain. e-mail: juanjose.cabrera@ulpgc.es

www.hh.um.es. DOI: 10.14670/HH-18-750

Key words: Corneal ulcer, Amniotic membrane, Corneal histopathology, Biomaterial

Introduction

The outer fibrous tunica of the eye comprises the sclera and the cornea. The limbus serves as the transitional zone between the cornea (anterior) and the sclera (posterior). The cornea, positioned at the front of the eyeball and transparent in nature, facilitates the passage of light into the eye, thereby enabling vision. In mammals, the cornea comprises the external corneal epithelium, the corneal stroma, and internally, Descemet's membrane and endothelium (Maggs, 2009).

Corneal ulceration occurs when the corneal epithelium is breached, exposing the underlying corneal stroma. It ranks among one of the most prevalent eye diseases in veterinary ophthalmology and is particularly common in rabbits, as indicated by some authors (Andrew, 2002; Maggs, 2009). The disease is classified as one of the inflammatory keratopathies, which can manifest either as ulcerative or non-ulcerative. Clinical signs, possible treatments, and prognosis may vary according to the depth of the defect. It is important to note that depth is not the only factor affecting healing; bacterial or fungal contamination may also adversely affect treatment (Maggs, 2009).

In superficial ulcers, the absence of infection, the elimination of the original cause, and topical treatment usually suffice to resolve the condition (Maggs, 2009).

In cases of deeper ulcers complicated by bacteria or fungal involvement, resolving them may necessitate corneal surgery and the application of biomaterials (Xie et al., 2018; Gogova et al., 2020). Some examples of such materials include stem cell transplantation, the use of polymer membranes, oral mucosa, amniotic membrane, and porcine bladder, among others (Sorsby et

al., 1947; Arora et al., 2005; Lo et al., 2013).

The amniotic membrane has been shown to be an effective biological material for restoring conjunctival and corneal surfaces in both human and veterinary patients when used as graft material (Tejwani et al., 2007; Rosen et al., 2018; Costa et al., 2019). In transplantation (Che et al., 2019; Dragúňová et al., 2019), it can be employed either independently or in conjunction with other tissues, such as the umbilical cord. Additionally, it is applied in eye drops to facilitate corneal re-epithelialization yielding satisfactory results (Tighe et al., 2017; Murris et al., 2018).

The amnion possesses several advantageous properties including its anti-fibrotic, anti-angiogenic, anti-protease, and anti-inflammatory properties. These properties contribute to the reduction of neutrophil infiltration, lipid peroxidation, and keratocyte death, thereby preventing symblepharon formation and decreasing stromal inflammation (Tamhane et al., 2005; Tandon et al., 2011; Lo et al., 2013).

Advanced diagnostic imaging tests are employed to acquire the most precise and accurate information regarding an individual's eye condition. Optical coherence tomography (OCT) can provide cross-sectional or tomographic images of the eye with micrometric resolution. Anterior segment OCT (AS-OCT) is utilized for diagnosing corneal diseases or anomalies, such as dystrophies or foreign bodies, and their repair following specific eye surgeries, among other applications (Armarnik et al., 2019; Kuo and Lee, 2019; Wang et al., 2019). Furthermore, studies have demonstrated its effectiveness in assisting corneal and intraocular surgery, particularly in determining the dimension of a corneal biopsy (Schmidt et al., 2019; Shan et al., 2019).

Moreover, histopathology serves as a valuable tool for examining morphology and analyzing its indicators can shed light on healing mechanisms by providing morphological evidence of the reparative process in corneal ulcers, while also gauging the extent of inflammation and fibrosis (Raghunathan et al., 2017; Jie et al., 2018).

The objective of this study was to scrutinize the corneal healing process by intentionally inducing a controlled stromal defect using an amniotic membrane. This investigation aims to validate the membrane's application as a viable treatment in routine clinical ophthalmology and to find a reliable method for evaluating the reparative process.

To assess the procedure, clinical signs, OCT measurements and histopathology were assessed at different stages of the recovery process. Comparisons were drawn between the amniotic membrane placed over the stromal or epithelial side of the defect and the control eye, where no membrane was applied.

Table 1. Experimental model. Treatment Assignment.

Number of rabbits	Eye		Follow-up days*		
	Left	Right	7	15	30
9	AM in mode epithelial	Control	3	3	3
9	AM in mode stromal	Control	3	3	3

*: Data are treatments and frequencies. Distribution of individuals (n=18) in different groups (n=3), treatment assignment according to epithelial side (n=9) or stromal side (n=9) in the left eye of each individual (the OD always acts as a control), and follow-up time until euthanasia (7, 15, and 30 days).

Materials and methods

This study was verified and approved by the ethics committee of the University of Las Palmas de Gran Canaria (OEBA-ULPGC 08/2016).

Design

This clinical trial aimed to evaluate the effects of inserting an amniotic membrane (AM) into the eye for corneal recovery in rabbits. Eighteen healthy, adult New Zealand rabbits, in optimal physical condition, were involved in the study. The rabbits were divided into three groups of six individuals: “Group 1” (individuals 1-6), “Group 2” (7-12), and “Group 3” (13-18). Group 1 was sacrificed after the first week, Group 2 after two weeks, and Group 3 after four weeks. Measurements of total corneal thickness, maximum ulcer thickness, and central thickness were taken for each eye.

Treatments (mode de insertion of AM) were randomly assigned according to Table 1.

Surgical approach

All rabbits underwent anesthesia using a uniform protocol and prepared for sterile procedures. A controlled stromal defect was induced in 36 eyes. This keratectomy was performed with a 7 mm vacuum trephine (Clear-vue®, Moria, France) set at a depth of 200 microns, following the manufacturer's instructions.

A single 8 mm diameter and 0.2 mm thick layer of dehydrated human AM (Visio-Amtrix®, TBF-Tissue engineering, France) was applied exclusively over the defect to the left eye (OS). In half of the cases (1, 2, 3, 7, 8, 9, 13, 14, and 15), the epithelial side of the membranes made contact with the corneal stroma, while in the other half, the stroma of the defect was in contact with the stromal matrix of the amniotic membrane.

Tissue glue (OcuSeal®, Beaver-Visitec International, Waltham, MA) was used to adhere the membrane following the manufacturer's instructions. To prevent a corneal reaction, no stitches, flaps, or contact lenses were utilized to fix the membrane, allowing for the evaluation of inflammatory and reparative reactions without interference from suture material, as well as the assessment of external evolution.

Postoperative management

A topical antibiotic (Ofloxacin 0.3%; Exocin®, Allergan, Ireland) was applied every 12 hours to all subjects, in conjunction with artificial tears (Systane®, Alcon, USA) until complete epithelialization was achieved.

To prevent potential digestive issues caused by handling, analgesic therapy with buprenorphine (0.03 mg/kg), metoclopramide (0.5 mg/kg), and ranitidine (2 mg/kg) were administered every 12 hours for the first three postoperative days (given subcutaneously).

Clinical signs

Throughout the initial week and bi-weekly thereafter until the study's conclusion, all eyes underwent daily remote and slit-lamp observations. These assessments

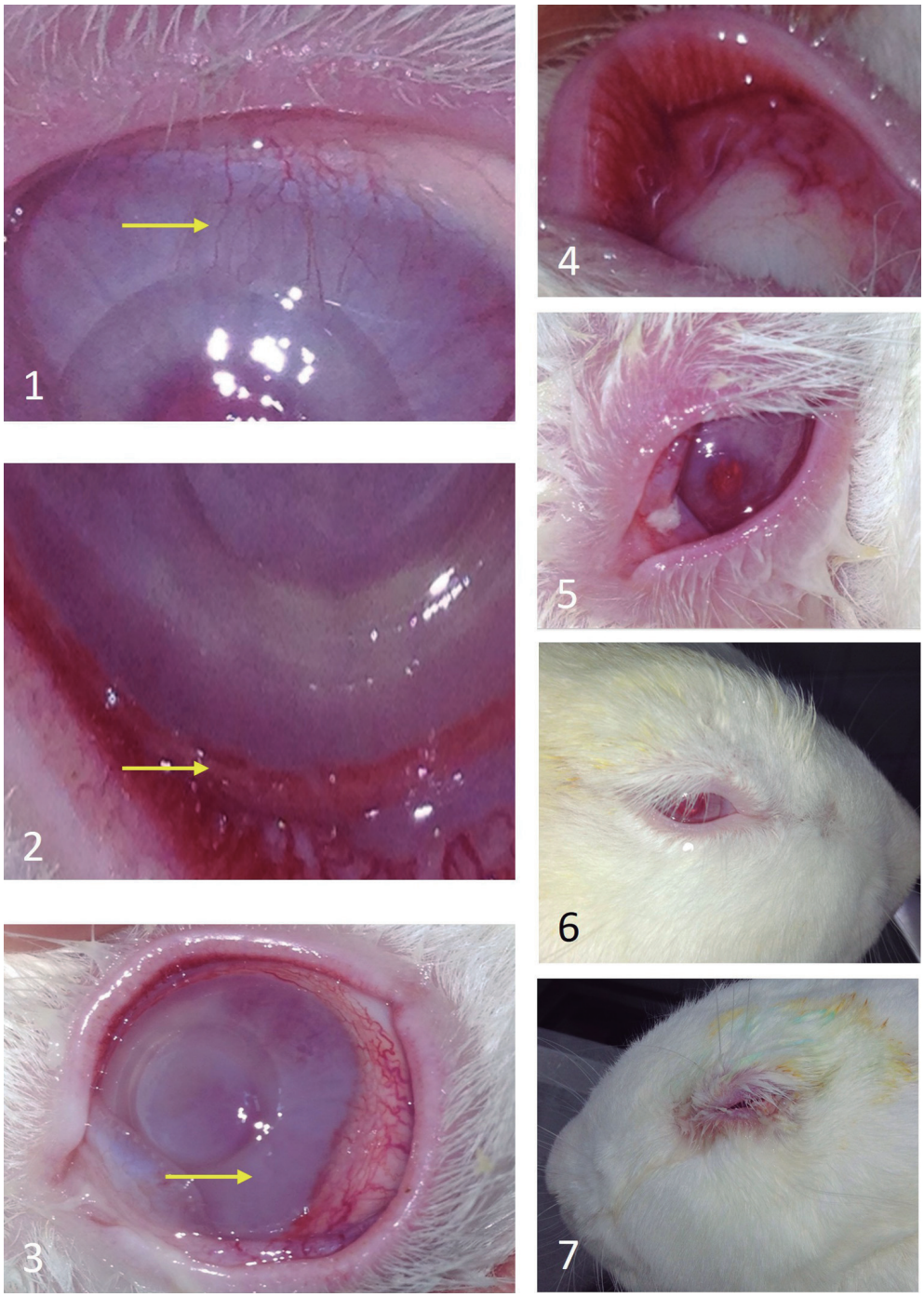

Fig. 1. Example of the different clinical signs studied. **1.** Superficial vascularization (arrow). **2.** Deep vascularization (arrow). **3.** Corneal edema (arrow). **4.** Conjunctival congestion. **5.** Secretion. **6.** Discomfort. **7.** Blepharospasm.

involved documenting the presence or absence of superficial and deep vascularization, discharge, discomfort, corneal edema, blepharospasm, hypopyon, and conjunctival congestion. (Fig. 1). The classification was assigned a value of "0" for the absence of a clinical sign, "1" for mild presentation, "2" for moderate presentation, and "3" for severe presentation.

OCT

On the specified date for each group, rabbits were euthanized and transconjunctival enucleation was performed on both eyes for subsequent OCT and histological analysis.

The OCT model employed in the present study was Stratus Cirrus 500®, Zeiss, Germany, operating in "anterior chamber" mode). Each cornea underwent several OCT examinations to derive average measurements, encompassing normal corneal thickness, maximum ulcer thickness (the maximum thickness adjacent to the keratectomy incision), and central thickness (the thickness in the middle of the keratectomy) (Fig. 2).

The OCT also provides information regarding the presence or absence of lesional and/or perilesional edema. According to their degree of edema, corneas were classified into four groups ranging from "0" (no edema) to "3". Perilesional edema was classified as "1" if the edema ranged from 400 to 500 microns, "2" if the edema ranged from 500 to 600 microns, and "3" if the edema exceeded 600 microns. For lesional edema, "1" denoted edema less than 400 microns, "2" for edema between 400 and 500 microns, and "3" for edema greater than 500 microns. (Fig. 2).

Histopathology

Following OCT analysis, the eyes were preserved and fixed in 4% buffered formaldehyde. Macroscopic sections were made at the level of the anterior chamber, encompassing the cornea, limbus, and lens. The cornea was sectioned centrally and embedded in paraffin. Four-micron sections were obtained and stained with hematoxylin and eosin (H&E).

In total, the 36 corneal samples underwent histological studies, with data collected from areas of the epithelium and stroma (central zone, intermediate zone between the center and one of the defects, and a point close to both defects). Additionally, the condition of the sclerocorneal limbus was also assessed.

Epithelium: For each of these areas, the following information was obtained: number of cell layers (numerical value), and the presence (1) or absence (0) of the basal layer and the basement membrane.

Stromal: keratocytes were studied and classified based on their activity at the stromal level, with a value (0) assigned to those without activity or mature keratocytes, typically found in lower strata of the corneal stroma and characterized by elongated, flat nuclei that are separated from one another. In contrast, keratocytes with larger elongated nuclei and appearing in greater numbers with less separation were identified as immature keratocytes with value (1), and the more active immature keratocytes with large nuclei and obvious nucleoli were identified as having value (2).

The same assessment was conducted at the stromal level determining the presence (1) or absence (0) of simple edema, myxoid edema, and capillary blood vessels.

For the sclerocorneal limbus: inflammation was assessed by examining the presence of lymphocytic infiltrates within the perivascular or interstitial spaces. Assigned values ranged from negative (0) to mild (1), moderate (2), and marked (3). The examination also included the presence (1) or absence (0) of neoformed capillaries as well as edema.

Histopathological data analysis

Using the data obtained from the histology section, a formula was developed that integrated all the data based on whether their presence and/or type contribute to corneal repair. The formula is outlined as follows:
Corneal repair= Epithelial regeneration+ Stromal repair+ Limbal repair.

For epithelial regeneration: data were collected at the different points described above (central zone, intermediate zone, proximal zone 1, and proximal zone 2). The number of cells (NCEL) is considered a positive value, with a higher count of cell layers indicating a more advanced level of regeneration. Additionally, basal cells (BCEL) and the presence of the basement membrane (BMEM) are considered positive values, reflecting enhanced regeneration. Therefore:

Epithelial regeneration= NCEL + BCEL + BMEM

Data related to stromal repair include the following: Concerning Keratocytes (KERAT), the degree of repair varies according to the stage. A value of "0" signifies the optimal condition. It is important to note that the presence of simple edema (EDEMA), myxoid edema (MIX), and vascularization (VASC) indicates a lower degree of repair. Accordingly:

Stromal Repair=KERAT (0>1>2) - EDEMA - MIX - VASC

In the case of limb repair, the following data are considered: Inflammation (LIMBUS_INFL): depending on the degree of inflammation, indicates varying levels of repair activity with a value of “0” denoting the highest level of repair. Vascularization (LIMBUS_VASC) and edema (LIMBUS_EDEMA): Their presence implies a lesser degree of repair. Therefore:

Limbal repair=LIMBUS_INF (0>1>2>3) - LIMBUS_ VASC - LIMBUS_EDEMA

Statistical analysis

Zero-inflated Poisson model

The impact of treatments on the progression of eye lesion counts in Blepharospasm, Discomfort, and Conjunctival congestion was assessed. However, the other clinical signs yielded too many null results, making them unanalyzable. Thus, for each marker, denoted as $N_{t,d,r,e}$ to represent the lesion count in eye "e" (right or left) corresponding to the r^{th} rabbit treated with "t" (Control, Epithelial, Stromal) on day "d" of follow-up. Given that most counts are null, they were modeled using a zero-inflated Poisson mode. Additionally, considering repeated measures within each rabbit, we included the rabbit effect as a random effect, nested within, which is the eye effect (Hall, 2000). The resulting zero-inflated mixed model for each marker (Blepharospasm, Discomfort, and Conjunctival congestion) is as expressed as

$$[MI]: N_{t,d,r,e} = \begin{Bmatrix} 0 & \text{with probability p} \\ \text{Poisson}\left(\mu_{t,d,r,e}\right) & \text{with probability } 1-p \end{Bmatrix}$$

being: $\ln(\mu_{t,d,r,e}) = \alpha + \beta d + \gamma_t + u_r + v_{e(r)}$

Here, γ_t represents the fixed effect of treatment (Control is taken as reference and thus, $\gamma_{Control} = 0$), $u_r \sim N(0,\sigma^2)$ denotes the random effect of the rabbit and $v_{e(r)}$ is the random effect of eye "e" nested in the rabbit "r". Additionally, we assume that the probability of zeros

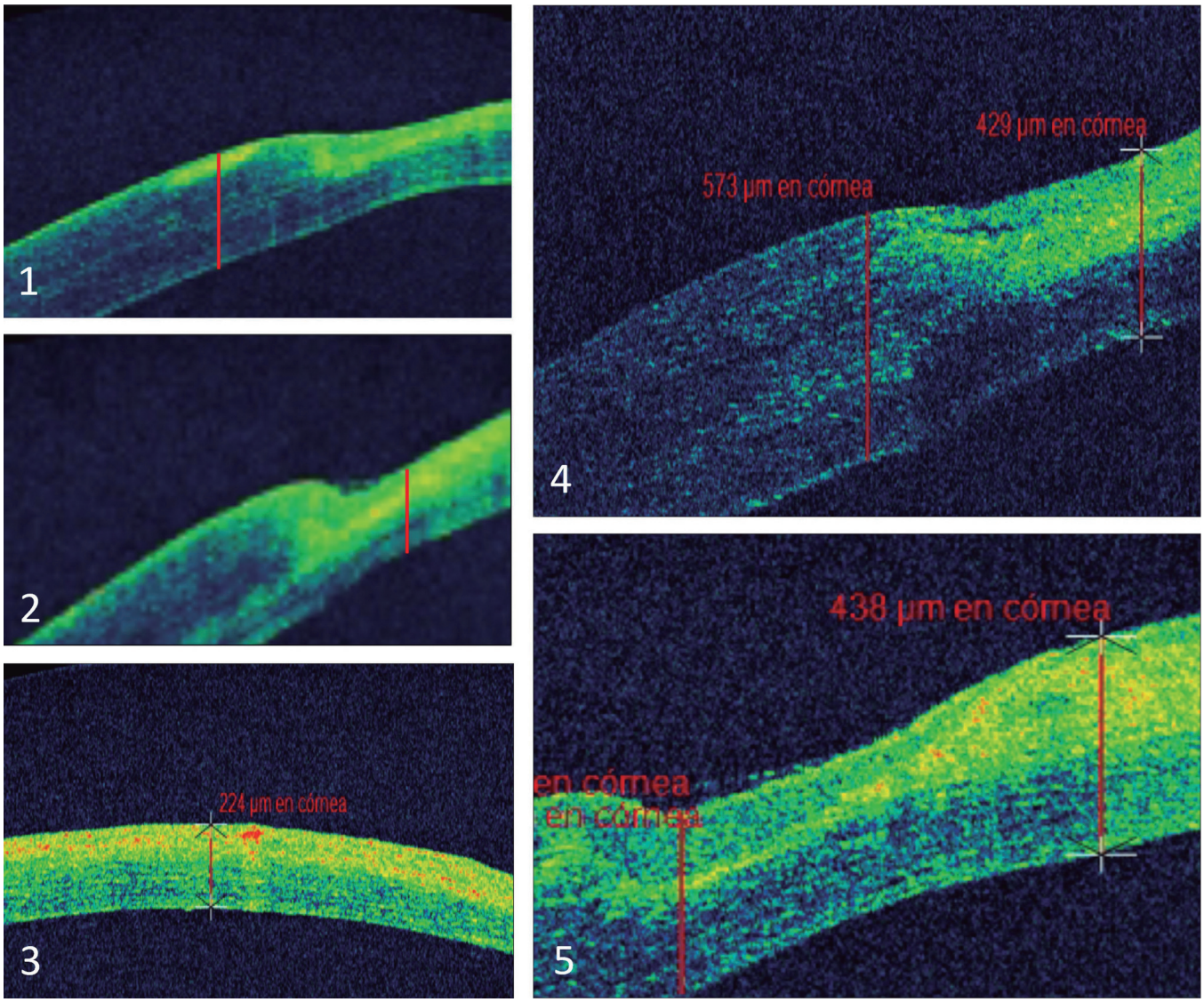

Fig. 2. Different OCT measurements. **1.** Normal corneal thickness. **2.** Maximum ulcer thickness. **3.** Central thickness. **4.** Perilesional edema. **5.** Lesional edema.

p_d may depend on the day of observation, with a higher probability towards the end of the follow-up.

OCT

In the study of OCT measurements, the variables were summarized as medians according to the week, eye, and mode of placement of the AM (epithelial and stromal).

Corneal repair score

We propose a corneal repair score as a weighted average of the three repair markers, namely: epithelial, stromal, and limbus repairs. Thus, for both eyes, the corneal repair score is defined as a convex linear combination in the form:

$$\text{Corneal.Repair} = w_1 \cdot \text{R. Epitelial} + w_2 \cdot \text{R. Stroma} + w_3 \cdot \text{R. Limbus}$$

To determine the coefficients w_1, w_2, w_3, we consider the difference:

$$D = \text{Corneal. Repair}_{\text{Left}} - \text{Corneal. Repair}_{\text{Right}}$$

Since the right eye was used as a control in all cases, D measures the effect of AM in its two modes of insertion in the left eye (epithelial and stromal) on corneal repair relative to the control (right eye). Thus, we refer to D as the superiority of the AM inserted in the left eye *versus* the control (right eye). Therefore, comparisons between treatments will be carried out using D-differences according to the following model:

$$D = \mu + \alpha \cdot AM + \beta \cdot Period + \gamma \cdot AM \times Period + Error \quad [M2]$$

Here, "AM" represents the factor denoting the insertion mode of AM, with epithelial and stromal modes coded as 1 and 0, respectively (stromal is taken as reference), "Period" takes values of 0 or 1 based on the first or 2-4 weeks and "Error" denotes the random variables corresponding to unexplained variability. We assume that these variables are independent and normally distributed with a mean of zero and standard deviation σ.

We choose the weights w_1, w_2, w_3, as those that maximize the adjusted-R^2 coefficient corresponding to the fit of the model [M2] using the least squares method. It is important to note that γ represents the effect of the interaction between AM and Period factors (AM concurrence in the epithelial mode with the second period).

The model was estimated using least squares and summarized by parameter estimates and standard errors (SE). Adjusted means for the differences D by period and mode of insertion of the AM were also estimated. Due to the low sample size, parameters were estimated

Table 2. Estimation of the zero-inflated Poisson models.

Marker	Effect	Coefficient (SE)	*P*-value
Blepharospasm	(Intercept)	0.88 (0.21)	<0.001
	Days (β)	-0.57 (0.06)	<0.001
	Treatment (γ_t)		
	Control (reference)	0	-
	AM in mode epithelial	0.48 (0.21)	0.02
	AM in mode stromal	-0.44 (0.27)	0.102
Discomfort	(Intercept)	0.96 (0.20)	<0.001
	Days (β)	-0.54 (0.05)	<0.001
	Treatment (γ_t		
	Control (reference)	0	-
	AM in mode epithelial	0.37 (0.20)	0.063
	AM in mode stromal	-0.44 (0.25)	0.083
Conjunctival congestion	(Intercept)	1.32 (0.14)	<0.001
	Days	-0.42 (0.03)	<0.001
	Treatment (γ_t)		
	Control (reference)	0	-
	AM in mode epithelial	0.18 (0.15)	0.24
	AM in mode stromal	-0.36 (0.18)	0.048

For Blepharospasm, Discomfort, and Conjunctival congestion, the lesion counts decrease throughout the follow-up period (*P*<0.001). Regarding Blepharospasm, the epithelial insertion mode was consistently associated with a higher expected number of lesions compared with the control (*P*=0.02) throughout the follow-up, while the stromal insertion mode showed no significant difference with the control (*P*=0.102). For Discomfort, although statistical significance was not reached, the expected lesion count in the nonconforming group tended to be higher when inserting the amniotic membrane in the epithelial mode relative to the control (*P*=0.063) and lower than the control when inserted in stromal mode (*P*=0.083). For Conjunctival congestion, the expected number of lesions was significantly reduced relative to the control for the stromal insertion mode (*P*=0.048), while the epithelial insertion mode showed no significant difference from the control (*P*=0.24).

using 90% confidence intervals.

Statistical significance was set at $P<0.05$. Data were analyzed using the R package, version 4.2.1 (R Development Core Team, 2022). The zero-inflated Poisson model was estimated using R-package "glmmTMB" (https://github.com/glmmTMB/glmmTMB). The model for the differences in corneal repair (D) was analyzed using R-package "emmeans" (https://cran.r-project.org/web/packages/emmeans/index.html).

Results

Clinical signs

Data were collected by one investigator. All 18 specimens were scanned and data collected daily from days 1 to 7. Scans were performed on days 7, 9, 11, and 15 for the second group (rabbits 7-12). In Group 3 (rabbits 13-18), scans were conducted on days 17, 21, 23, 27, and 30.

Table 2 summarizes the estimation of the fixed effects corresponding to the zero-inflated Poisson model. For the three markers (Blepharospasm, Discomfort, and Conjunctival congestion), the lesion counts showed a consistent decrease throughout the follow-up period ($P<0.001$). Regarding Blepharospasm, the epithelial insertion mode was consistently associated with a higher expected number of lesions compared to the control throughout the follow-up ($P=0.02$), while the stromal insertion mode did not exhibit a significant difference from the control ($P=0.102$). Although statistical

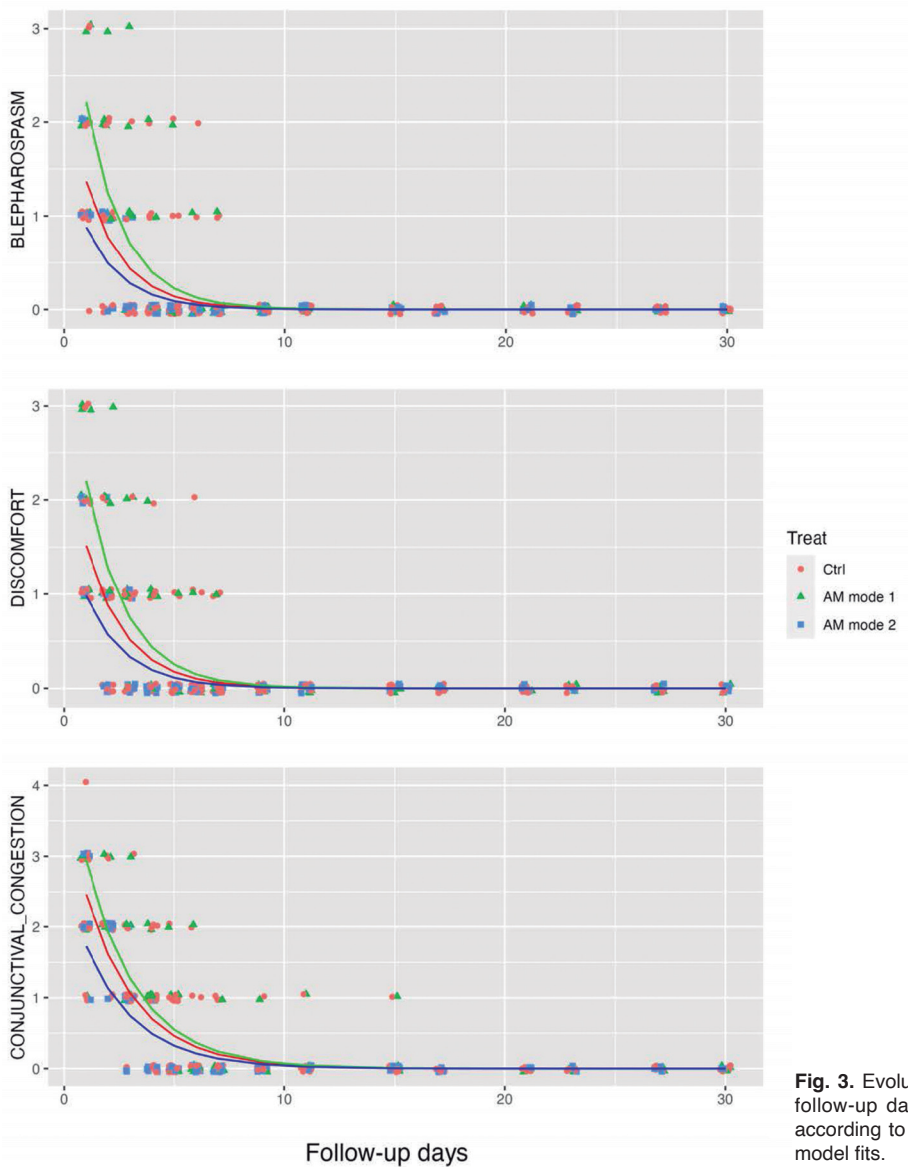

Fig. 3. Evolution of lesion counts according to treatment and follow-up day. For each marker, evolution of lesion counts according to treatment. The curves correspond to the mixed-model fits.

significance was not achieved, the expected lesion count in the nonconforming group tended to be higher when the AM was inserted in the epithelial mode compared with the control (P=0.063) and lower than the control when inserted in the stromal mode (P=0.083). For the conjunctiva, the expected number of lesions was significantly reduced relative to the control for the stromal insertion mode (P=0.048), while the epithelial insertion mode showed no significant difference from the control (P=0.24). These results are illustrated in Figure 3.

OCT

According to the measurements performed, different results were obtained concerning corneal thickness and the presence and type of edema.

Table 3. Corneal thickness according to treatment mode and week.

		Mode of insertion of the amniotic membrane (AM)			
		Epithelial N=9		Stromal N=9	
Thickness	Week	Left eye	Right eye	Left eye	Right eye
Total	1	413	483	422	470
	2	452	464	454	453
	4	427	422	429	429
Ulcer	1	272	219	259	234
	2	379	320	344	290
	4	285	273	254	245
Central	1	283	343	296	256
	2	368	306	418	409
	4	325	336	301	288

Descriptive table summarizing the corneal thicknesses in medians for each eye according to the week of observation and the method of amniotic membrane insertion in the left eye of each rabbit. Data are medians.

Table 4. Statistical analysis of the lesional and perilesional edema.

			Eye with the amniotic membrane	
Week	Edema	Control eye	≤400	>400
1	Peri-lesional	≤400	0	0
		>400	0	3
2		≤400	0	0
		>400	0	2
4		≤400	0	0
		>400	0	1
1	Lesional	≤400	1	0
		>400	1	1
2		≤400	0	1
		>400	0	2
4		≤400	4	0
		>400	0	2

No statistically significant differences were found when comparing the control eye with the test eye over time. Data are frequencies.

Several OCT measurement results could not be obtained for all eyes: in Group 1 at 4OD and 6OD for total thickness (TT) and central thickness (CT); in Group 2 at 7OS, 8OD, and 8OS for TT; 8OD for Ulcer Max Thickness (UMT) and in 8OD and 8OS for CT.

The characteristics of corneal thickness by eye and follow-up are summarized in Table 3, which presents median values of corneal thicknesses in each eye at different points of the keratectomy: the normal corneal thickness (total), ulcer maximum thickness (ulcer max), and central thickness (central). This summarization is organized based on the week of observation and the method by which the AM was inserted in the left eye of each rabbit. Throughout the follow-up period, thicknesses between the two eyes did not exhibit statistically significant differences, possibly due to small sample sizes.

The same occurs with Table 4, which presents the statistical analysis of lesional and perilesional edema. Over time, no statistically significant differences were observed between the control and study eyes.

Histopathology

Table 5 summarizes the variations in corneal repair scores (epithelial, stromal, and limbal) between the two eyes, considering the mode of AM implantation and the week of follow-up.

In this table, it is noted that when evaluating differences in corneal repair (left minus right eye) based on the treatment group, the epithelial repair of the first week exhibits an almost statistically significant difference between the methods of membrane placement (P=0.077).

Figure 4 illustrates the findings of most cases in Group 1 during the first week of treatment. The presence of stromal reactivity and irregular regenerated

Table 5. Differences in corneal repair (left eye minus right eye) according to treatment group.

		AM insertion mode		
	Week	Epithelial N=9	Stromal N=9	*P*-value*
Epithelial	1	0 (-3; 1.5)	10 (10; 12.5)	0.077
	2	1 (-3; 12)	-3 (-10; 4)	0.7
	4	-2 (-2.5; 6)	-1 (-2; 0)	1
Stroma	1	1 (0.5; 2)	1 (0.5; 4)	1
	2	2 (1; 2)	0 (0; 0.5)	0.346
	4	0 (-0.5; 2)	0 (-1.5; 1.5)	0.825
Limbo	1	-1 (-1; -0.5)	-1 (-1.5; -0.5)	0.814
	2	0 (-0.5; 0)	0 (-0.5; 0)	1
	4	0 (0; 0)	0 (-0.5; 0)	0.505

Data are medians (25-75th percentile). *: Wilcoxon test for independent samples. When examining variations in corneal repair (left eye minus right eye) based on treatment groups, a statistically significant difference was observed in epithelial repair during the first week, with a *P*-value of 0.077 indicating the impact of the method of membrane placement.

epithelium, in the membrane epithelial side (A), contrasts with the absence of such features in image (B) corresponding to the cornea with the membrane placed on the stromal side in OS, exhibiting a mature stroma. Below, control case (C) with scant epithelium can be observed. The limbal area shows marked habitual activity (D).

The score of the corneal repair model leading to the best fit [M2] was:

Corneal.Repair = 0.0675×R. Epitelial + 0.195×R. Stroma + 0.7375×R. Limbus

The analysis of the effects of AM on corneal repair is summarized in Tables 6 and 7. In the first week, the expected value of the repair score was higher when the stromal insertion mode was used compared with the control (superiority of AM-stromal score vs. control=0.570; 90% CI=0.021; 1.119). However, in the second period, the insertion in epithelial mode was superior to the control (difference in scores=0.397; 90% CI=0.009; 0.785). Finally, when the insertion modes are directly compared, the stromal mode shows greater effectiveness in the first period (superiority of AM-epithelial score vs. stromal=0.869; 90% CI=-1.655; -0.093) while in the second period, the epithelial mode is more effective than the stromal mode (superiority of AM-epithelial score vs. stromal=0.745; 90% CI=0.197; 1.294).

Figure 5 illustrates the evolution of corneal repair in

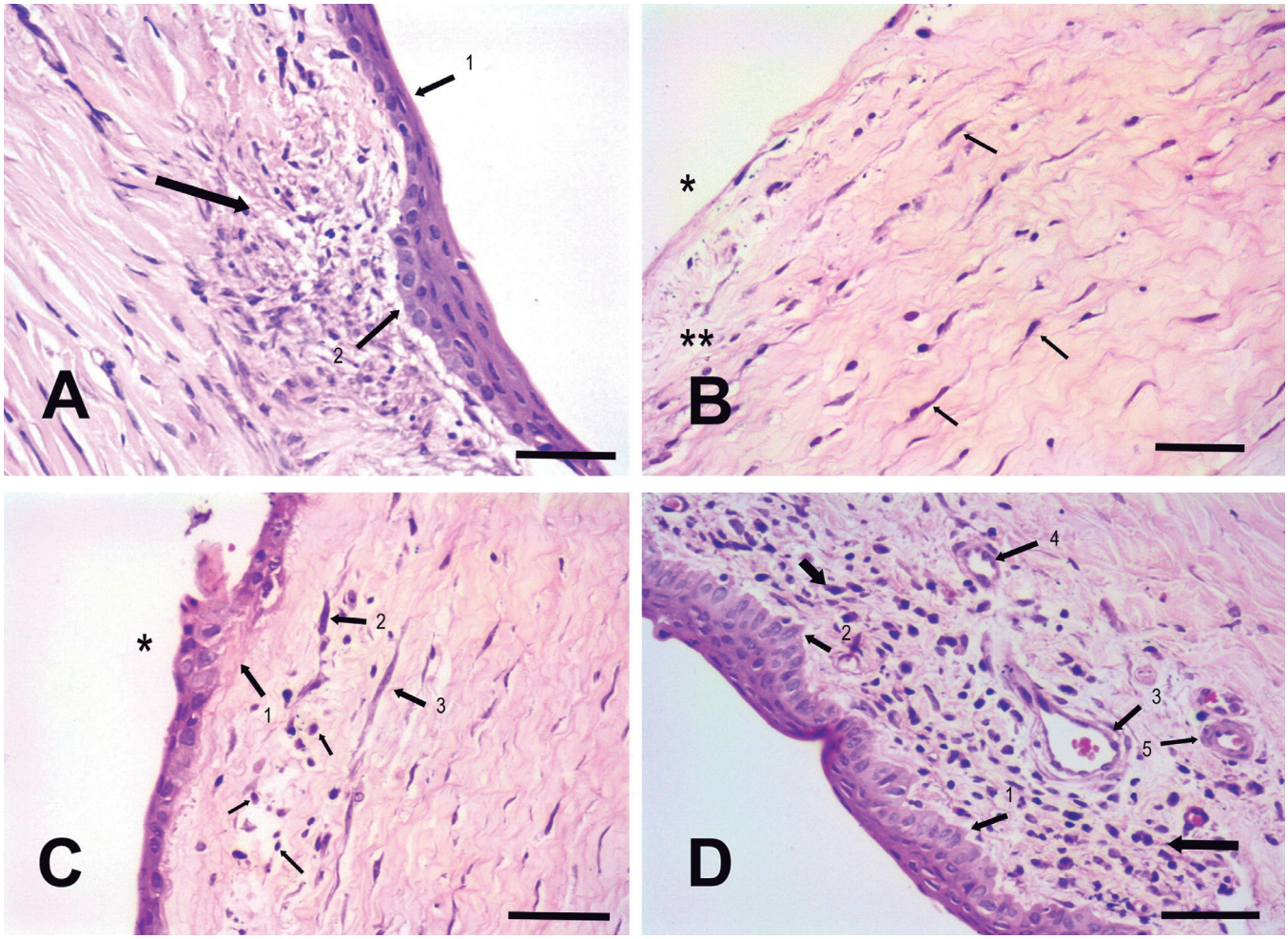

Fig. 4. Histopathological section of corneas corresponding to Group 1. **A.** OS. Membrane placed on the epithelial side. High stromal reparative activity in the proximal area of the surgical wound: thick arrow; asterisk*: normal stroma. Irregular number of epithelium layers and altered basal cells: thin arrows 1, 2. H&E. **B.** OS. Membrane placed on the stromal side. Cornea with absent epithelium: (asterisk). Lax stroma with superficial and myxoid edema: (double asterisk). Immature keratocytes in the stroma: (arrows). H&E. **C.** OD Control. Cornea with two or three layers of reactive epithelium: (asterisk). Irregular basal cells and imprecise basement membrane: (arrow 1). Reactive keratocytes: (arrows 2, 3) Sparse inflammatory cells into lax stroma with myxoid edema: (small arrows). H&E. **D.** OS. Limbus. Area of the corneal limbus with non-specific chronic inflammatory signs: (thick arrows). Regular basal cells: (arrows 1, 2). Capillary vessel in formation structure: (arrow 3). Two conformed capillaries: (arrows 4, 5). Well-formed epithelium: (asterisk). H&E. Scale bars: A, D, 50 μm; B, C, 70 μm

Groups 2 and 3. One case with the membrane placed on the epithelial side (A) in mode 1 in OS showed a high, regenerated epithelium with residual active stroma, whereas, in image (B), there is a well-formed epithelium and stroma with immature keratocytes and aqueous edema. The control case (C). The limbus exhibits an apparent structure and moderate activity (D).

Discussion

It is well known that rabbits are commonly used in laboratory research due to their manageability, space efficiency, and cost-effectiveness. Since domestic rabbits (Oryctolagus cuniculus) are popular pets, they are frequently encountered in veterinary practice. As prey species, rabbits have prominent, laterally positioned eyes that provide them with a wide field of vision (Maggs, 2009).

Extensive research has been conducted on ocular alterations in wild animals, pets, and experimental animals, with the cornea being the most commonly affected organ and corneal ulcers being the most common pathology in this species (Andrew, 2002).

Clinical signs

Different studies have reported different results on the reduction of pain after AM transplantation in various corneal diseases. A study of patients with acute ocular burns (Tamhane et al., 2005) found that patients undergoing amniotic transplantation did not experience as much pain as those receiving only medical therapy. Comparatively, our study found that the eye with AM (OS) exhibited more signs of pain, including greater discomfort, conjunctival congestion, and blepharospasm than the OD, as shown in table 2, and figure 3. The statistical results for the three clinical signs indicate $P<0.001$.

The placement of the membrane predetermined differences as to its location: blepharospasm and discomfort were more common in patients with the membrane in the epithelial position than in those with the membrane in the stromal position, although discomfort was not statistically significant ($P=0.063$). These results may correlate with the sensation of a foreign body in patients with Sjögren's syndrome who have undergone amniotic membrane transplantation (AMT) (Shafer et al., 2019).

Another factor to consider when determining whether AMT is more advantageous than other techniques or treatments is the recovery of visual acuity. Accordingly, several studies have demonstrated that there is no statistically significant difference in visual acuity improvement or signs that may alter it, such as

Table 6. Linear model with treatment-week interaction for the difference *D* in proposed corneal repair score between left and right eyes (left minus right).

	Coefficient (SE)	*P*-value
(Intercept)	0.570 ± 0.312)	0.089
Mode of insertion of the AM		
Stromal	0 (Reference)	
Epithelial	-0.869 (0.441)	0.069
Period		
Week 1	0 (Reference	
Weeks 2 and 4	-0.918 (0.382)	0.03
Interaction: epithelial mode of insertion and weeks 2-4*	1.615 (0.540)	0.01

*: The treatment-period interaction leads to the fact that in the first period, AM is more effective in stromal mode while in the second period, it is more effective in epithelial mode. This table summarizes the estimation of the corresponding linear model, showing statistical significance for the period-implant mode interaction ($P=0.010$).

Table 7. Adjusted means [90% CI†] deduced from the linear model (Table 6).

	Mode of insertion of the AM		
Period	Stromal*	Epithelial*	Epithelial vs Stromal**
Week 1	0.570 [0.021; 1.119]	-0.299 [-0.848; 0.250]	-0.869 [-1.645; -0.093]
Weeks 2 and 4	-0.348 [-0.736; 0.040]	0.397 [0.009; 0.785]	0.745 [0.197; 1.294]

*: Difference in corneal repairs between the left and right eyes; adjusted means assess the superiority of AM in both modes (left eye) relative to the control (right eye). **: Comparison of the epithelial and stromal insertion modes: superiority of the epithelial mode insertion minus superiority of the stromal mode AM. †: Since the sample size was small, 90% confidence intervals were used. This table confirms, through the confidence interval, that corneal repair is superior in both modes (OS) compared with the control (OD). It also demonstrates that in the second period (weeks 2 and 4), insertion in the epithelial mode relative to the stromal mode leads to a marked superiority of 0.745 (90% CI).

opacity or corneal edema, after acute ocular burn (Tamhane et al., 2005), alkali burn (Subasi et al., 2017), or following pterygium surgery (Akbari et al., 2017).

However, several authors have observed differences in visual acuity when comparing the use of AM with different techniques to treat recalcitrant filamentous fungal keratitis (Chen et al., 2016) or bacterial stromal keratitis (Altay et al., 2016).

In this study, a statistical comparison of corneal edema presentation among the study subjects was not feasible due to the prevalence of numerous "0" or null results. Subsequent studies, potentially involving a larger number of individuals, should be undertaken to yield insights into visual recovery outcomes.

Several methods have been described for placing the AM with varying results. A meta-analysis type study published in 2019 (Liu et al., 2019) revealed that there are differences in vision improvement rates (VIR) depending on the technique used to cover the ulcer: the highest VIR was found in cases where the AM was placed in a single layer, followed by those whose AM was placed in a multilayer technique, and those with the lowest VIR were the "sandwich" group. In the present study, the unilayer technique was used. Future studies may provide further insight into the differences between different techniques and the severity of ulcer complications.

The presence of corneal vascularization was examined in a study where AMT was implanted one month after performing a superficial chemical keratectomy. Significant differences were found between the experimental and control groups three months after

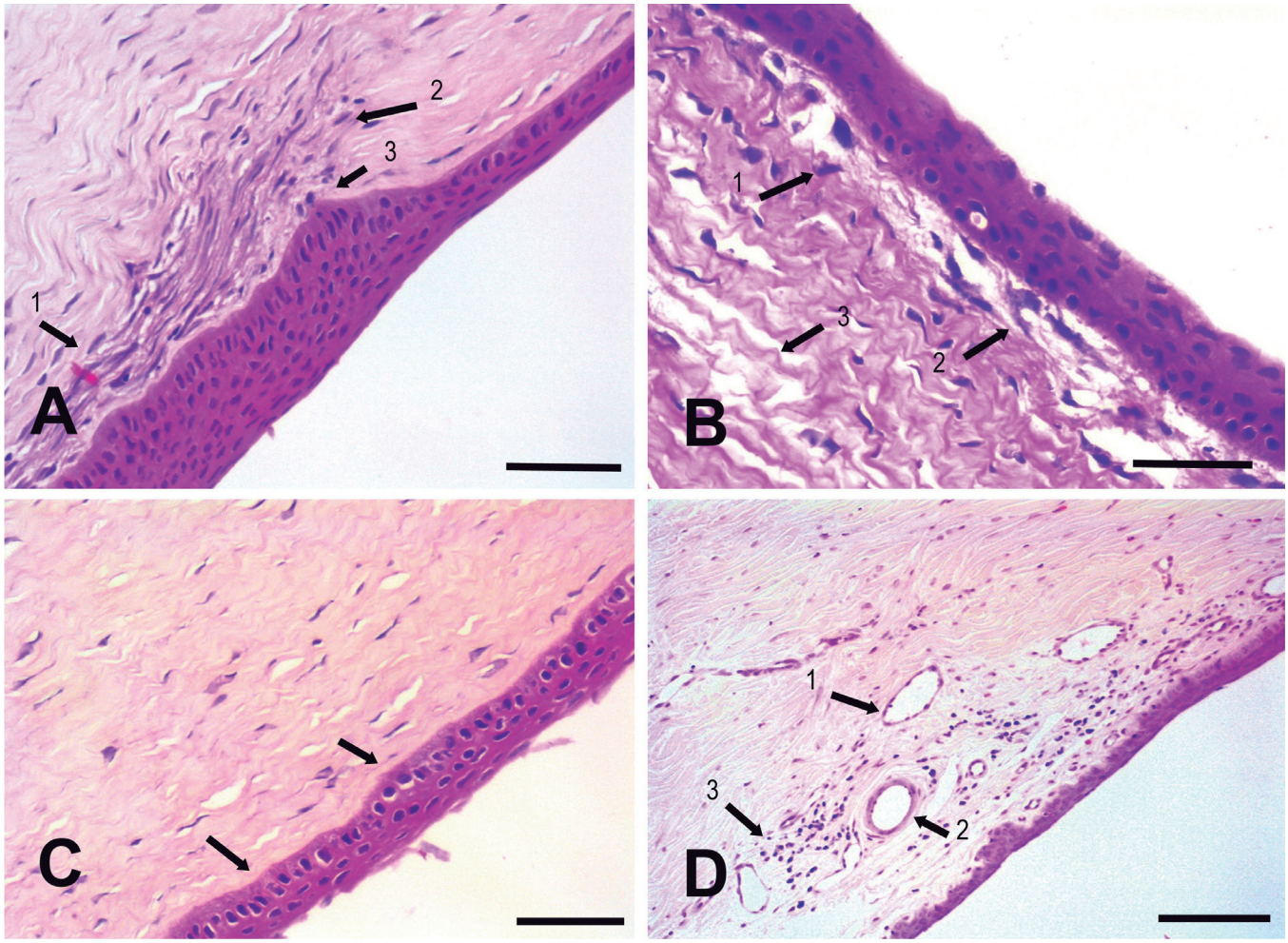

Fig. 5. Histopathological section of corneas corresponding to Groups 2 and 3. **A.** OS. Membrane placed on the epithelial side. Wound area with dense stroma with active keratocytes: (arrows 1, 2). High epithelium and well-formed basal layer: (arrow 3). H&E. **B.** OS. Membrane placed on the stromal side. Well-formed epithelium with more than five layers with moderately preserved basal cells. Corneal stroma with immature and active keratocytes surrounded by interstitial aqueous edema: (arrows 1, 2, 3). H&E. **C.** OD. Control. Epithelium with several layers. Irregular basal cell layer and visible basement membrane: (arrows). Stroma with mature keratocytes, light edema, and no vessels: (asterisks). H&E. **D.** OD. Limbus. General view of the limbus area, with conformed capillaries: (arrows 1, 2) moderate edema and some infiltrating lymphocytes: (arrow 3). H&E. Scale bars: A, D, 70 μm; B, 50 μm; D, 100 μm.

the keratectomy (Kim and Tseng, 1995).

In a study by Tandon et al. (2011), the results were consistent regarding vascularization presentation, since no difference was found between the placement of an AMT or not for corneal vascularization factors in patients with moderate ocular burns.

Similarly, Tamhane evaluated the combination of AMT with medical treatment for ulcers caused by burns, specifically moderate and severe. Their findings revealed no statistically significant differences in the manifestation of vascularization between the groups, aligning with our study, where no statistically significant distinction between groups was detected for this characteristic (Tamhane et al., 2005). It is worth noting that vascularization was observed in both groups three months after initiating the study. In a study carried out by Subasi (Subasi et al., 2017), they examined the effects of AMT on rabbit corneas affected by alkali burns. Vascularization was evaluated in a manner similar to our work, not only using the AMT technique but also comparing it with crosslinking (CXL) and the combination of both. In terms of vascularization, a significant difference was found between groups, with the group receiving AMT as the sole treatment and the group receiving AMT combined with CXL showing the highest degree of vascularization (Subasi et al., 2017).

In this study, like with edema and other clinical signs, we were unable to carry out statistically reliable comparisons between the eye where the AM was placed and the control, as well as between different placement modes. We suggest conducting additional studies to delve deeper into this factor, which we deem highly significant and has been extensively discussed by numerous authors.

Corneal repair

Several authors have employed the recovery of corneal thickness as a factor in evaluating the efficacy of AMT. This can be measured using various methods, including OCT, which was utilized in the current study (Raghunathan et al., 2017; Che et al., 2019; Costa et al., 2019).

The OCT technique has been employed for determining thickness measurements in different areas of the cornea, providing reliable diagnostic reproducibility, for cornea-specific results (Das et al., 2019; Duman et al., 2019). Despite this, there have only been a few studies in which this technology has been used to evaluate corneal regeneration (Raghunathan et al., 2017).

In the present study, as presented in Table 3, the highest measurements were obtained in the corneas evaluated in the second week after keratectomy. These values decreased in the third group (week four) but remained higher than those of the first week, except for three measurements (TT OD, TT OS, and CT OD), indicating some recovery of the defect.

A similar trend was observed in Raghuthan et al.'s study (2017), where maximum corneal values were found in the initial days and then decreased. It is noteworthy, however, that in our study, we found a greater thickness during the second week rather than the first (Table 3). The presence of corneal edema may be the cause of this condition.

Therefore, in our work, the use of AMT evaluated by OCT as demonstrated in Table 3 did not indicate an improvement in corneal thickness recovery.

The present study defines corneal repair as the sum of epithelial regeneration and stromal and limbal repair. Without using immunohistochemical techniques, the data used were obtained from the histopathological study. Each of these three components has its own factors that influence corneal repair as a whole, either positively or negatively.

To our knowledge, this definition of corneal repair has not been employed previously. Nevertheless, various authors describe the process using terms like corneal regeneration or corneal recovery, considering factors like re-epithelialization or the restoration of corneal thickness, which are integrated into this novel formula.

In numerous studies, re-epithelialization has been identified as a factor in corneal recovery. AMT has been employed as a therapeutic intervention for various types of ulcers and their underlying causes, encompassing ulcers induced by burns (Tamhane et al., 2005), ulcers exhibiting different levels of severity (Tandon et al., 2011), and ulcers infected by multiple microorganisms (Altay et al., 2016). Moreover, this terminology is encountered in research studies where AMT is applied in conjunction with alternative surgical methods (Akbari et al., 2017) or implemented through diverse placement approaches (Liu et al., 2019).

According to the literature consulted, re-epithelialization is determined by external slit lamp examination and fluorescein staining assessment (Tandon et al., 2011; Altay et al., 2016; Akbari et al., 2017), whereas in the present study, it was determined by histological analysis and the corneal repair formula.

Based on our results, we propose that corneal repair is a more comprehensive term than those typically used to describe corneal recovery. No distinctions were noted between groups when exclusively examining clinical signs and OCT measurements in this study. Furthermore, even upon scrutinizing histological images alone, it remains inconclusive whether there is an improvement with the membrane's use or if one placement side is superior to the other.

Nevertheless, the outcomes derived from the new formula suggest that, as illustrated in Tables 6 and 7, corneal repair is more effective with the application of AM when compared with the control eye. Specifically, the initial repair, occurring within the first week, showed superiority in individuals with the membrane placed on the stromal side (AM-stromal score vs. control=0.570; 90% CI=0.021; 1.119). Conversely, during the extended recovery period (weeks 2 and 4), individuals with the AM placed on the epithelial side exhibited better corneal

repair (difference of scores=0.397; 90% CI=0.009; 0.785).

These results were confirmed when directly comparing the insertion modes (difference of epithelial score vs. stromal=-0.869; 90% CI=-1.655; -0.093) in the first week, while in the second period, the superiority of epithelial score vs. stromal=0.745; 90% CI=0.197; 1.294.

All the analysis suggests that, in the first week, AMT is more effective in stromal mode, while in the long term, the epithelial mode is more effective. This aligns with different articles indicating that AMT results in an improvement in corneal thickness recovery. However, most articles use combinations of AM with other techniques such as cross-linking (Soeken et al., 2018), the multilayer technique (Costa et al., 2019), or even combining the multilayer technique with other techniques such as mixed gas C3F8 in the anterior chamber (Fan et al., 2016) or the addition of corneal stromal cells between layers of ultrathin AM (González-Andrades et al., 2017).

The present study utilized a monolayer TMA technique, demonstrated to be fully effective by Goktas et al. (Goktas et al., 2017). However, further research is necessary to substantiate its use, including investigating various methods of applying the AM in terms of positions, times, and surgical techniques. Additionally, exploring the application of the new formula for corneal repair in different corneal conditions is essential.

Conclusion

Our findings suggest that the use of AM with the unilayer technique enhances corneal healing after a controlled-depth corneal defect. In a short recovery period, placing the membrane on the stromal side yields better results, while in the longer term, positioning it on the epithelial side demonstrates superior outcomes in terms of corneal recovery. Therefore, we propose the use of a statistical formula based on a combination of histopathological results to measure corneal recovery. To our knowledge, this is the first time it has been employed and it may offer a more accurate and reliable method than the observation of clinical signs and the measurement of corneal thickness by OCT.

Disclosure of funding received. Our research was funded by the European Society of Veterinary Ophthalmology; ESVO Grant 2016.
Conflict of interest. Authors have no conflict of interest to declare.

References

Akbari M., Soltani-Moghadam R., Elmi R. and Kazamnejad E. (2017). Comparison of free conjunctival autograft *versus* amniotic membrane transplantation for pterygium surgery. J. Curr. Ophthalmol. 29, 282-286.

Altay Y., Tamer S., Burcu A. and Balta Ö. (2016). Amniotic membrane transplantation in bacterial and herpetic stromal keratitis. Turk. J. Med. Sci. 46, 457-462.

Andrew S.E. (2002). Corneal diseases of rabbits. Vet. Clin. Exot. Anim. 5, 341-356.

Armarnik S., Minouni M., Goldenberg D., Segev F., Meshi A., Segal O. and Geffen N. (2019). Characterization of deeply embedded corneal foreign bodies with anterior segment optical coherence tomography. Graefes Arch. Clin. Exp. Ophthalmol. 257, 1247-1252.

Arora R., Mehta D. and Jain V. (2005). Amniotic membrane transplantation in acute chemical burns. Eye 19, 273-278.

Che X., Wu H., Jia C., Sun H., Ou S., Wang J., Jeyalatha M.V., He X., Yu J., Zuo C., Liu Z. and Li W. (2019). A novel tissue-engineered corneal stromal equivalent based on amniotic membrane and keratocytes. Invest. Ophthalmol. Vis. Sci. 60, 517-527.

Chen Y., Gao M., Duncan J.K., Ran D., Roe D.J., Belin M.W. and Wang M. (2016). Excisional keratectomy combined with focal cryotherapy and amniotic membrane inlay for recalcitrant filamentary fungal keratitis: A retrospective comparative clinical data analysis. Exp. Ther. Med. 12, 3014-3020.

Costa D., Leiva M., Sanz F., Espejo V., Esteban J., Vergara J., Díaz C., Huguet E., Cairó M., Ríos J. and Peña M.T. (2019). A multicenter retrospective study on cryopreserved amniotic membrane transplantation for the treatment of complicated corneal ulcers in the dog. Vet. Ophthalmol. 22, 695-702.

Das M., Menda S.A., Panigrahi A.K., Pranja N.V., Yen M., Tsang B., Kumar A., Rose-Nussbaumer J., Acharya N.R., McCulloch C.E., Lietman T.M., McLeod S.D. and Keenan J.D. (2019). Repeatability and reproducibility of slit lamp, optical coherence tomography, and scheimpflug measurements of corneal scars. Ophthalmic Epidemiol. 26, 251-256.

Dragúňová J., Kabát P., Cucorová V., Hajská M. and Koller J. (2019). Deep frozen amniotic membrane used as a scaffold and/or carrier for different cell types. Cell Tissue Bank. 20, 35-48.

Duman R., Edtekin T., Duman R., Aslan E., Sabaner M.C. and Cetinkaya E. (2019). The novel model: Experimental optical coherence tomography-guided anterior segment imaging chick embryo model. Indian J. Ophthalmol. 67, 54-58.

Fan J., Wang M., and Zhong F. (2016). Improvement of amniotic membrane method for the treatment of corneal perforation. Biomed. Res. Int. 2016, 1693815.

Gogova S., Leiva M., Ortillés A., Lacerda R.P., Seruca C., Laguna F., Crasta M., Ríos J. and Peña M.T. (2020). Corneoconjunctival transposition for the treatment of deep stromal to full-thickness corneal defects in dogs: A multicentric retrospective study of 100 cases (2012-2018). Vet. Ophthalmol. 23, 450-459.

Goktas S.E., Katircioglu Y., Celik T. and Ornek F. (2017). Surgical amniotic membrane transplantation after conjunctival and limbal tumor excision. Arq. Bras. Oftalmol. 80, 242-246.

González-Andrades M., Mata R., González-Gallardo M.D.C., Medialdea S., Arias-Santiago S., Martínez-Atienza J., Ruiz-García A., Pérez-Fajardo L., Lizana-Moreno A., Garzón I., Campos A., Alaminos M., Carmona G. and Cuende N. (2017). A study protocol for a multicenter randomized clinical trial evaluating the safety and feasibility of a bioengineered human allogeneic nanostructured anterior cornea in patients with advanced corneal trophic ulcers refractory to conventional treatment. BMJ Open 7, e016487.

Hall D.B. (2000). Zero-inflated poisson and binomial regression with random effects: a case study. Biometrics 56, 1030-1039.

Jie J., Yang J., He H., Zheng J., Wang W., Zhang L., Li Z., Chen J., Jeyalatha M.V., Dong N., Wu H., Liu Z. and Li W. (2018). Tissue

remodeling after ocular surface reconstruction with denuded amniotic membrane. Sci. Rep. 8, 6400.

Kim J.C. and Tseng S.C. (1995). The effect on inhibition of corneal neovascularization after human amniotic membrane transplantation in severely damaged rabbit corneas. Korean J. Ophthalmol. 9, 32-46.

Kuo Y.C. and Lee Y.C. (2019). A CARE-compliant article: optical coherence tomography for epithelial basement membrane dystrophy: A case report. Medicine 98, e15032.

Liu J., Li L. and Li X. (2019). Effectiveness of cryopreserved amniotic membrane transplantation in corneal ulceration: A meta-analysis. Cornea 38, 454-462.

Lo K., Kohanim S., Trief D. and Chodosh J. (2013). Role of amniotic membrane transplantation in acute chemical injury. Int. Ophthalmol. Clin. 53, 33-41.

Maggs D.J. (2009). Córnea y Esclera. In: Slatter, Fundamentos de Oftalmología Veterinaria. 4th ed. Maggs D (ed). Elsevier Barcelona. pp 179-208.

Murris M.S., Moshirfar M., Birdsong O.C., Ronquillo Y.C., Ding Y. and Hoopes P.C. (2018). Amniotic membrane extract and eye drops: a review of literature and clinical application. Clin. Ophthalmol. 18, 1105-1112.

Raghunathan V.K., Thomasy S.M., Strom P., Yañez-Soto B., Garland S.P., Sermeno J., Reilly C.M. and Murphy C.J. (2017). Tissue and cellular biomechanics during corneal wound injury and repair. Acta Biomater. 58, 291-301.

Rosen R. (2018). Amniotic membrane grafts to reduce pterygium recurrence. Cornea 37, 189-193.

R Core Team (2022). R: A language and environment for statistical computing. R Foundation for Statistical Computing, Vienna, Austria. URL https://www.R-project.org/

Schmidt E.M., Stiefel H.C., Houghton D.C. and Chamberlain D. (2019). Intraoperative optical coherence tomography to guide corneal biopsy: A case report. Cornea 38, 636-641.

Shafer B., Fuerst N.M., Massaro-Giordano M., Palladino V., Givnish T., Macci I., Sulewski M.E., Orlin S.E. and Bunya V.Y. (2019). The use of self-retained cryopreserved amniotic membrane for the treatment of Sjögren syndrome: a case series. Digit. J. Ophthalmol. 25, 21-25.

Shan J., De Boer C. and Xu B.J. (2019). Anterior segment optical coherence tomography applications for clinical care and scientific research. Asia Pac. J. Ophthalmol. 8, 146-157.

Soeken T.A., Zhu H., DeMartelaere S., Davies B.W., Kim M., Wang H.C., Aden J., Grimm R., Alt C., Kochevar I.E. and Johnson A.J. (2018). Sealing of corneal lacerations using photoactivated rose bengal dye and amniotic membrane. Cornea 37, 211-217.

Sorsby A., Haythorne J. and Reed H. (1947). Further experience with amniotic membrane grafts in caustic burns of the eye. Br. J. Ophthalmol. 31, 409-418.

Subasi S., Altintas O., Yardimoglu M., Yazir Y., Karaman S., Rencber S.F. and Kavram K. (2017). Comparison of collagen cross-linking and amniotic membrane transplantation in an experimental alkali burn rabbit model. Cornea 36, 1106-1115.

Tamhane A., Vajpayee R., Biswas N.H., Pandey R.M., Sharma N., Titiyal J.S. and Tandon R. (2005). Evaluation of amniotic membrane transplantation as an adjunct to medical therapy as compared with medical therapy alone in acute ocular burns. Ophthalmology 112, 1963-1969.

Tandon R., Gupta N., Kalaivani M., Sharma N., Titiyal J. and Vajpayee R.B. (2011). Amniotic membrane transplantation as an adjunct to medical therapy in acute ocular burns. Br. J. Ophthalmol. 95, 199-204.

Tejwani S., Kolari R.S., Sangwan V.S. and Rao G.N. (2007). Role of amniotic membrane graft for ocular chemical and thermal injuries. Cornea 26, 21-26.

Tighe S., Moein H.R., Chua L., Cheng A., Hamrah P. and Tseng S.C.G. (2017). Topical cryopreserved amniotic membrane and umbilical cord eye drops promote re-epithelialization in a murine corneal abrasion model. Invest. Ophthalmol. Vis. Sci. 58, 1586-1593.

Wang S.B., Cornish E.E., Grigg J.R. and McCluskey P.J. (2019). Anterior segment optical coherence tomography and its clinical applications. Clin. Exp. Optom. 102, 208-217.

Xie H.T., Zhang Y.Y., Jiang D.L., Wu J., Wang J.S and Zhang M.C. (2018). Amniotic membrane transplantation with topical interferon alfa-2b after excision of ocular surface squamous neoplasia. Int. J. Ophthalmol. 11, 160-162.

Accepted April 18, 2024